Study of Inverter Control Strategies on the Stability of Low-Inertia Microgrid Systems

Preprint

Jing Wang and Govind Saraswat

National Renewable Energy Laboratory

Presented at the IEEE Power and Energy Society General Meeting
Denver, Colorado
July 17–21, 2022

NREL is a national laboratory of the U.S. Department of Energy
Office of Energy Efficiency & Renewable Energy
Operated by the Alliance for Sustainable Energy, LLC

This report is available at no cost from the National Renewable Energy Laboratory (NREL) at www.nrel.gov/publications.

Contract No. DE-AC36-08GO28308

Conference Paper
NREL/CP-5D00-81403
July 2022

Study of Inverter Control Strategies on the Stability of Low-Inertia Microgrid Systems

Preprint

Jing Wang and Govind Saraswat

National Renewable Energy Laboratory

Suggested Citation
Wang, Jing, and Govind Saraswat. 2022. *Study of Inverter Control Strategies on the Stability of Low-Inertia Microgrid Systems: Preprint*. Golden, CO: National Renewable Energy Laboratory. NREL/CP-5D00-81403. https://www.nrel.gov/docs/fy22osti/81403.pdf.

NREL is a national laboratory of the U.S. Department of Energy
Office of Energy Efficiency & Renewable Energy
Operated by the Alliance for Sustainable Energy, LLC

This report is available at no cost from the National Renewable Energy Laboratory (NREL) at www.nrel.gov/publications.

Contract No. DE-AC36-08GO28308

Conference Paper
NREL/CP-5D00-81403
July 2022

National Renewable Energy Laboratory
15013 Denver West Parkway
Golden, CO 80401
303-275-3000 • www.nrel.gov

NOTICE

This work was authored in part by the National Renewable Energy Laboratory, operated by Alliance for Sustainable Energy, LLC, for the U.S. Department of Energy (DOE) under Contract No. DE-AC36-08GO28308. This material is based upon work supported by the U.S Department of Energy, Advanced Research Projects Agency – Energy under grant DE-AR0001016. The views expressed herein do not necessarily represent the views of the DOE or the U.S. Government.

Cover Photos by Dennis Schroeder: (clockwise, left to right) NREL 51934, NREL 45897, NREL 42160, NREL 45891, NREL 48097, NREL 46526.

Study of Inverter Control Strategies on the Stability of Low-Inertia Microgrid Systems

Jing Wang and Govind Saraswat
Power Systems Engineering Center, National Renewable Energy Laboratory, Golden, CO 80401, USA
jing.wang@nrel.gov, Govind.Saraswat@nrel.gov

***Abstract*— This paper investigates the stability of low-inertia microgrid systems with two control strategies that have different percentages of grid-forming (GFM) inverters. The first control strategy has approximately 50% GFM inverters, and all the battery inverters are working in GFM control mode. Originally, the second control strategy has approximately 10% GFM inverters, with only two battery inverters working in GFM control mode and the rest working in grid-following (GFL) PQ control mode based on current control, which cannot stabilize the microgrid system. Then, the second control strategy is modified to change the GFM inverters from droop control to isochronous control and the GFL battery inverters from traditional current control to voltage control for power control. Both control strategies can maintain system stability; however, the first control strategy can better handle contingency events. The study indicates that 1) a microgrid system with a higher percentage of GFM inverters has better stability; and 2) a microgrid with a lower percentage of GFM inverters can have poor stability, but improved control strategies in inverters can improve system stability. This study improves the understanding of how different percentages of GFM inverters and inverter control strategies affect the system stability of low-inertia microgrids.**

***Index Terms*—Droop control, grid-forming control, grid-following control, voltage and frequency stability.**

I. Introduction

Grid-forming (GFM) inverters are becoming a critical asset to maintain system stability and resilience, especially for future electric grids that will have massive amounts of distributed energy resources (DERs), which will replace traditional synchronous generation and become the dominant generation source [1]. Extensive research efforts have focused particularly on GFMs for microgrid systems with low inertia and high penetrations of DERs. An inverter-dominant microgrid including a synchronous generator in parallel with both GFM and grid-following (GFL) inverters is studied in [2] to investigate the system stability and dynamics with different control strategy combinations of either or both types of inverters. Power control strategies of GFM inverters for microgrid applications are studied in [3] to design the power control algorithm for GFMs to allow them to inject power in grid-connected mode and to form the system voltage and frequency in islanded mode using voltage control. And in [4], a unified, droop-free, secondary control framework using a single communication strategy is developed for both GFL and GFM inverters to regulate the system voltage and frequency to nominal values based on distributed optimization.

Further, some existing work has evaluated the dynamic interactions of GFM and GFL inverters on the stability of low-inertia power systems [5], [6], analyzed the stability of systems with GFM and GFL inverters [7], studied the frequency fluctuation impacts of droop-controlled inverters [8], and learned the type and power level of the influence of the operated load on microgrid transient stability [9]. Although extensive research has been performed on GFM inverters, there is a lack of studies on how different percentages of GFM inverters and inverter control strategies affect the system stability of low inertia microgrids with significant amounts of GFM and GFL inverters under varying load and solar irradiance conditions.

Therefore, the goal of this paper is to fill this research gap and provide a useful reference for power system engineers on choosing the correct control strategy for inverters in microgrids. The contributions of this paper are summarized as follows: 1) Two control strategies of a microgrid—one with 50% GFM inverters and one with only 10% GFM inverters—are investigated against a real-world microgrid system with large amounts of GFM and GFL inverters and varying load and solar irradiance conditions to study the stability of a microgrid system in a realistic scenario. 2) The microgrid system with only two GFM inverters is found to be unstable because any small changes in frequency can cause instability; thus, a strategy with these two GFM inverters working in isochronous mode and changing the traditional current-controlled GFL inverter to a voltage-controlled GFL inverter is developed to stabilize the system. 3) Strategy I, which has more GFM inverters, shows better stability than Strategy II, which has fewer GFM inverters, thus demonstrating the benefits of using GFM controls in a microgrid. 4) A microgrid system with a low percentage of GFM inverters can have poor stability but improving the control strategies in the inverters can improve system stability.

II. Microgrid System Under Study

A. Description of the Microgrid System

The microgrid system under study is based on a real power network at the University of Minnesota, which has many buildings with multiple DERs (GFM and GFL inverters), controllable loads, and noncontrollable loads. A single-line diagram of the campus microgrid is presented in Fig. 1. The names "csCIu," "CCu3," "MOB," etc., refer to the buildings. Note that the photovoltaic (PV) inverters always

This work was authored by the National Renewable Energy Laboratory, operated by Alliance for Sustainable Energy, LLC, for the U.S. Department of Energy (DOE) under Contract No. DE-AC36-08GO28308 This material is based upon work supported by the U.S Department of Energy, Advanced Research Projects Agency – Energy under grant DE-AR0001016. The views expressed in the article do not necessarily represent the views of the DOE or the U.S. Government. The U.S. Government retains and the publisher, by accepting the article for publication, acknowledges that the U.S. Government retains a nonexclusive, paid-up, irrevocable, worldwide license to publish or reproduce the published form of this work, or allow others to do so, for U.S. Government purposes.

operate in GFL mode, and the battery inverters can operate in either GFL mode or GFM mode. In this paper, the microgrid always operates in islanded mode because our focus is on the stability of the islanded microgrid system with multiple GFM and GFL inverters. Note that the diesel generator works in PQ control mode to inject active and reactive power into the grid rather than in VF control to form the system voltage. The power capacity ratings of the DERs and load are listed in Table 1. More details on the power system model can be found in [10][11].

The model is developed and simulated in eMEGASIM of the real-time simulator, OPAL-RT, with a simulation time step of 100 µs. Each DER unit has an implemented detailed control algorithm, such as a phase-locked loop (PLL), droop control, voltage, and current control. The noncontrollable loads and cold load are modeled as constant impedance loads. The controllable loads in each building are modeled as dynamic PQ loads receiving power profiles.

To simulate such a complex power system model with a small time step, the model is separated into five groups using the ARTEMiS-SSN nodal interface block in the OPAL-RT ARTEMiS library. The locations of the SSN block are marked by the dark blue box, as shown in Fig. 1. The general principle is to have the partitioned subsystem with less than two buildings and less than 10 single-phase switches. Note that the V-type (left and right) interface is selected because the partitioned subsystems are connected to the rest of the system through a line impedance that is inductive.

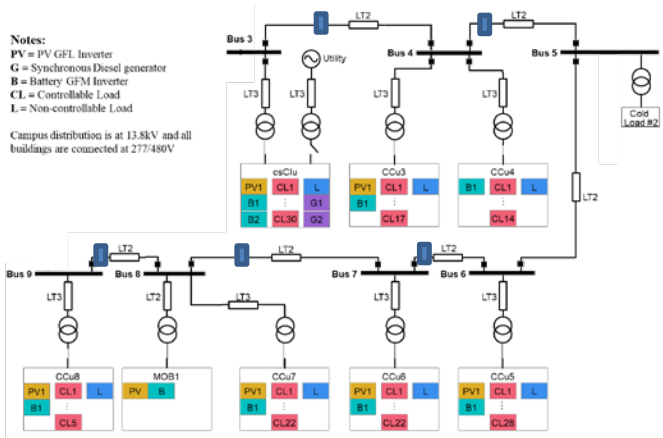

Fig. 1. Schematic diagram of the simulated microgrid in OPAL-RT.

Table 1. Net Load Resource Power Capacity Ratings

Type	Resource Power Capacity (kVA)								
	csClu	CC u3	CC u4	CC u5	CCu 6	CC u7	CC u8	MOB 1	Cold Load 2
PV1	100	50	-	100	100	50	100	25	-
PV2	-	-	-	-	-	-	-	25	-
B1	100	25	300	80	200	200	50	100	-
B2	100	-	-	-	-	-	-	-	-
G1/ G2	50	-	-	-	-		-	-	-
L	250	30	35	30	40	25	30	-	200
CL	500	300	315	300	360	225	270	-	-

** **B**: Battery, **G**: Diesel generator, **L**: Noncontrollable load, **CL**: Controllable load

B. *Control Strategies of Inverters*

For this islanded microgrid system, two control strategies are investigated: 1) *Strategy I: 50% GFM inverters*: All battery inverters work in GFM mode with power sharing by droop control; and 2) *Strategy II: 10% GFM inverters*: Two battery inverters have the largest capacity as the GFM sources (the battery inverters in CCu4 and CCu7), and the rest of the battery inverters operate in GFL mode. Note that the PV inverters work in GFL mode in both strategies. Strategy I represents future grid operations, with the GFL inverters changing to GFM mode to support and form electric grids. Strategy II represents the traditional style of grid operations, in which two GFM inverters operate in parallel, sharing power as the master and the GFL inverters as the slaves. The percentage of GFM inverters is calculated based on the capacity of the total GFM inverters to the capacity of the total DER generation.

1) *Strategy I: 50% GFM Inverters*

All the GFM inverters use the voltage control algorithm discussed in [12]. The benefit of this GFM inverter control mode over the traditional double-loop voltage control mode is that it shapes the output of the inverters (capacitor voltage) as a stiff voltage source without an output impedance. This design is particularly important for a system that has many DERs to cancel out the interactions between inverters for better stability and reliability. Because the GFM inverters have different capacities, the droop coefficients (m_p and n_q) of the inverters are calculated based on their capacities. The load in the islanded microgrid system varies based on the load profile, which affects the system voltage and the frequency because the GFM inverters are load-following units. Moreover, a GFM inverter with an LCL filter controls the capacitor bank voltage to nominal; however, the inductance connected with the external grid can cause a nonnegligible voltage drop and result in low voltage at the terminal (e.g., 0.95 p.u.). To guarantee that the system voltage and frequency stay close to the nominal values with varying load, secondary control offsets, $\Delta\omega$ and ΔV, are added to each GFM inverter. The same $\Delta\omega$ is added to all GFM inverters, whereas ΔV is individually tuned because it is impossible to achieve perfect reactive power sharing. This might not be standard practice for many commercial inverters today; however, it is necessary to consider compensation techniques to improve the frequency and voltage drops caused by droop and power sharing. In this strategy, there are 9 GFM inverters and 8 GFL inverters, and each building has at least 1 GFM inverter.

2) *Strategy II: 10% GFM Inverters*

The straightforward way is to change the GFM inverters to GFL inverters based on the model in Strategy I and leave the battery inverters in CCu4 and CCu7 in GFM control mode; however, the system is unstable when the load varies, and the two GFM inverters struggle to reach new operation points of frequency and voltage. The simulation test shows that a slight change in system frequency results in stability issues for the GFL inverter even though the system frequency is within the safe operating limits. In this strategy, with 2 GFM inverters and 14 GFL inverters, the offset compensation is no longer a viable solution. Based on the test results, with only 2 GFM inverters establishing the system voltage and frequency and the rest of the inverters following the grid voltage, we can conclude that the islanded microgrid does not have enough GFM capability. This is also explained in [5], which notes that GFM inverters have significant advantages over GFL inverters, particularly in systems that have a large number of inverter-based sources, and the available system inertia drops.

To make Strategy II work, the control algorithm of all the GFL battery inverters is modified from GFL control to GFM control for active and reactive power tracking, as suggested in [3]. In this case, the inverter-level control adopts VF control with self-generated voltage and frequency. The control schematic diagram is shown in Fig. 2. The control mode selection is used to enable/disable the integrator in droop control. If it is grid-connected for active and reactive power injection, the integrator is enabled; otherwise, the integrator is disabled for islanded mode. Note that disabling P^* and Q^* is optional in islanded mode. Using droop control for both grid-connected and islanded mode and the same voltage control for inverter device-level control completes the goal of using the same control structure for the GFM inverter without needing to switch between the GFL current control and the GFM voltage control modes; however, applying this power tracking in islanded mode might not work well because in an islanded system, the system frequency, ω_o, is not equal to the fundamental frequency, ω^*, due to the droop control and power sharing of the GFM inverters. This results in the active power being unable to accurately track its power reference ($P \neq P^*$). Similarly, the reactive power cannot accurately track its power reference ($Q \neq Q^*$).

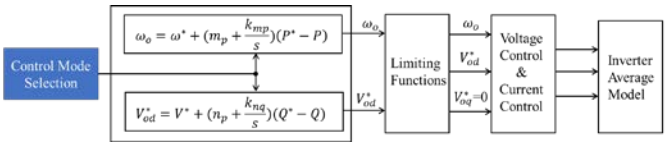

Fig. 2. Schematic diagram of the GFM inverter working in PQ control mode and power sharing.

To achieve active power tracking with GFM control, the two GFM inverters adopt the isochronous control mode without power sharing. Each inverter uses a fixed voltage and a frequency as the references. This maintains the system frequency in the islanded microgrid at the nominal level, and the battery inverters can accurately track the active power and provide GFM capability to their terminal buses.

III. Inverter Modeling and Control

The inverter control strategy determines the dynamics and stability of the inverter. Two major control schemes—GFL and GFM—are commonly adopted in grid-connected inverters. Fig. 3 summarizes different inverter control strategies.

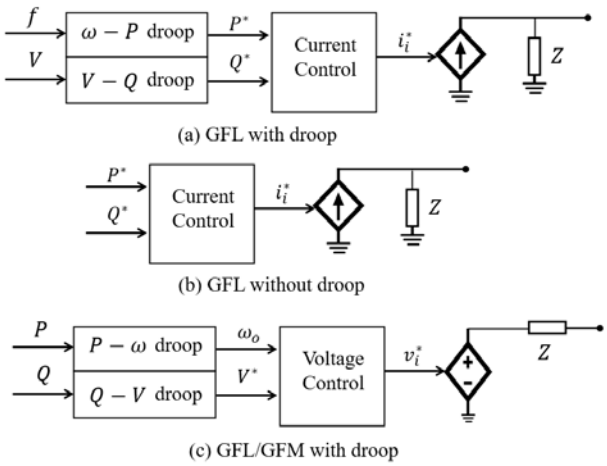

Fig. 3. Different inverter control schemes: (a) GFM with droop, (b) GFM without droop, and (c) GFL/GFM with droop.

Fig. 3 (a) and (b) show GFL control with and without droop, respectively, and Fig. 3 (c) shows GFL/GFM control with droop, which is the new design, as described in Strategy II in Section II. The GFL control schemes shown in Fig. 3 (a) and (b) are traditional designs, which need the grid voltage for synchronization; thus, a PLL is used for this purpose. The GFL control scheme shown in Fig. 3 (c) does not require a PLL for grid synchronization; however, a sync-check block with an active synchronization function is usually used in the inverter control logic to close the circuit breaker of the inverter when its terminal voltage is in sync with the grid voltage [13].

For this study, all GFL and GFM inverters are based on a simplified average simulation model. The following two subsections provide details on the control algorithms.

A. Grid-Forming Control

The GFM control algorithm used in this study references the control design in [12]. The control diagram is presented in Fig. 4, which includes three major components:

- Active and reactive power control. This is a typical droop control mode, and the output is the frequency reference and the d-component of the voltage control loop. The frequency is used to create the phase angle for the *d-q* Park transformation.
- Outer voltage control. The voltage control uses the inverse dynamic model control, which achieves the closed-loop transfer function equal to the unity gain: $v_{od} = v_{od}^*, v_{oq} = v_{oq}^*$. All the internal and external dynamics to the inverter are canceled out, and this inverter has a no-delay response to the input signals.
- Inner current control. The same as the voltage control loop, this current control loop also uses the inverse dynamic model control, and the closed-loop transfer function is equal to the unity gain: $i_{id} = i_{id}^*, i_{iq} = i_{iq}^*$.

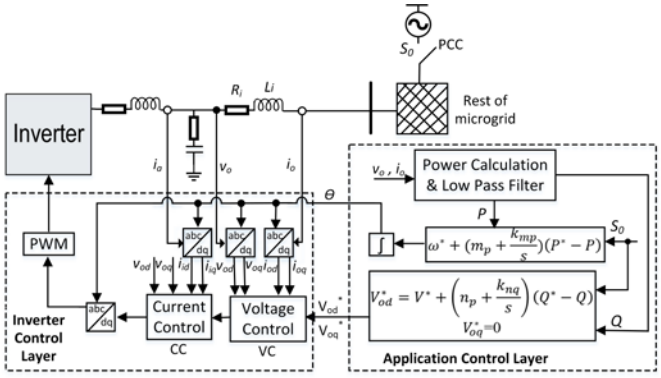

Fig. 4. Control diagram of the GFM inverter [12].

Note that the reference, v_{oq}^*, is always set to zero, as shown in Fig. 4. The active and reactive power droop can be modified based on the chosen control strategy. In Strategy I, all the battery inverters adopt this GFM control, and the integrator in the droop control is disabled for power sharing among the GFM inverters. In Strategy II, two chosen GFM inverters disregard the droop control and use the fixed frequency and voltage references (isochronous mode) for the GFM control, and the rest of the battery inverters adopt the voltage control-based PQ control, with the integrators enabled for active and reactive power tracking. Because the two GFM inverters use isochronous mode, the voltage and

frequency of the islanded microgrid are at their nominal values. The rest of the GFL battery inverters, with voltage-controlled PQ control, as shown in Fig. 4, can generate the desired active and reactive power with better stability than by using current-controlled PQ control. The control parameters of the integrator (K_{mp} and K_{nq}) are very small (1×10^{-4}) to avoid transients and dynamics in the frequency and voltage, respectively.

B. Grid-Following Control

In this study, all PV inverters adopt the GFL control mode. They are smart inverters that can receive active and reactive power references for power tracking. Fig. 5 presents the control diagram of the GFL inverters. This is a commonly used control algorithm that mainly includes the PLL, the current reference generation, and the current control.

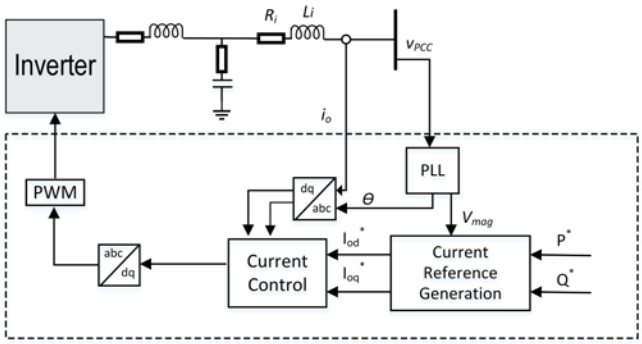

Fig. 5. Control diagram of the GFL inverter [14].

IV. Simulation Setup

In this real-time simulation, the controllable load in each building receives the time-series load profiles, and the PV inverters receive the time-series PV generation profiles as well. The load profiles are obtained through the metering system by the energy group of the University of Minnesota, and the data are interpolated with a 30-second resolution based on the 1-second resolution raw data for a 15-minute test. The PV generation profile is extracted based on the real-world solar irradiance data from the National Renewable Energy Laboratory's Solar Measurement and Instrumentation Data Center, and it is converted to the generation profile based on the PV capacity. The PV profile is taken from the time duration as the load profile, and it is interpolated into a 10-second resolution to show the impact of fast-changing solar irradiance on system stability. The load and PV profiles for the csCIu are presented in Fig. 6. The changing load and PV generations provide a good testing condition to evaluate the stability of the microgrid system using the two strategies.

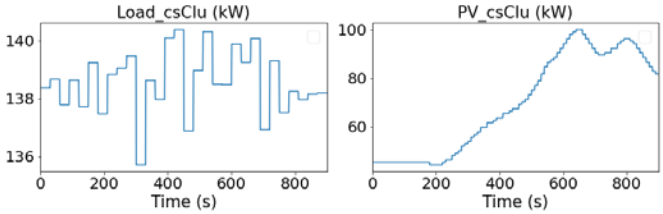

Fig. 6. The load (left) and PV (right) profiles of the csCIu.

The overall control and operation strategy of this islanded microgrid system has the GFM inverters operating in VF control mode to establish the system voltage and frequency and the GFL inverters operating in PQ control mode to serve the load. For the evaluation, the generation capacity and load demand are configured to be balanced to ensure system voltage and frequency stability. For this paper, there is no system-level energy management system (EMS) because the focus is to study the impact of different control strategies on the system stability with the low-inertia microgrid. With the EMS dispatching, the inverters might receive different set points for the two strategies. For a fair comparison of the two control strategies, all the testing conditions are kept the same, including the load profiles, the PV profiles, and the initial conditions (e.g., battery state of charge (SOC)).

V. Simulation Results

This section presents the real-time simulation results of the two strategies. The real-time simulation is 15 minutes, with the load profile updating every 30 seconds and the PV profile updating every 10 seconds. A test scenario with two contingency events is selected: 1) The first contingency event happens at CCu6, when the 200-kVA battery inverter is disconnected at 5 minutes. 2) The second contingency event happens at CCu8, when the 50-kVA battery inverter is disconnected at 11.5 minutes. We assume that all the batteries have SOCs higher than 80% and can discharge during the duration of the test. Representative results are presented in Figs. 7–10. Note that the legends in the figures are self-explained—for instance, in f_mob, *f* means frequency, and *mob* means the mobile building MOB1, as shown in Fig. 1.

A. Strategy I: All Battery Inverters in GFM Mode

As mentioned in Section II, each building has at least one GFM inverter that can form/establish the system voltage collectively. Droop control is used to share the active and reactive power proportionally among them, and the secondary control compensation is added to boost the system voltage and frequency close to nominal values. Fig. 7 (a) and (b) show the frequency and voltage of each building, respectively.

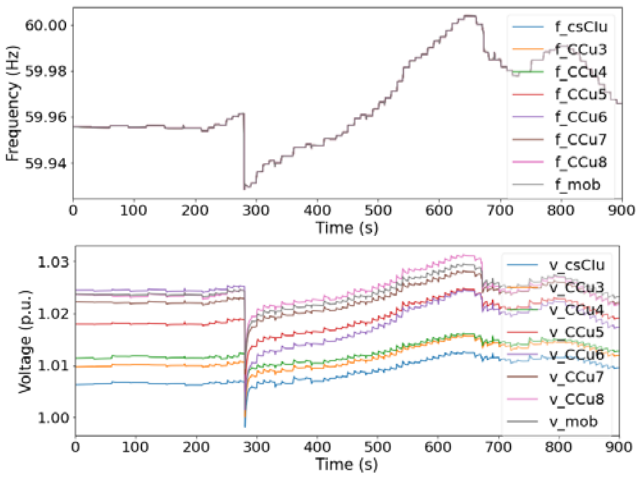

Fig. 7. Frequency (top) and voltage RMS (bottom) of all the buildings.

Fig. 7 (a) indicates that all the GFM inverters can achieve accurate active power to reach the same frequency. This is as expected because the GFM inverters must reach the same system frequency to stabilize the system. In the first contingency, the frequencies immediately drop approximately 0.04 Hz and slowly increase because the GFM inverters increase the active output power, and the active power generation from the PV units also increases. In the second

contingency, a GFM inverter with a smaller capacity is lost; thus, the frequency drop is smaller. The frequencies do not increase like they do in the first contingency because the active power generation from the PV units reduces due to the solar irradiance. It is obvious that the frequency dynamics are similar to the PV profile shown in Fig. 6 (b). This can be understood by the fact that the generation of the PV units affects the net load, which eventually affects the power sharing and the frequency dynamics.

Fig. 7 (b) shows the voltage root mean square (RMS) of all the buildings. It is clear that the voltage dynamics are similar to the frequency dynamics. When the first contingency event is applied, the voltages drop and then slowly increase following the dynamics of the PV generation. When the second contingency is applied, the system voltages drop slightly and continue to decrease because of the PV production. Overall, the two contingency events cause disturbances to the islanded system with little (near-zero) inertia, and together the GFM and GFL inverters can maintain the system voltage and frequency transient stability.

The results of the active and reactive power of each GFM inverter are presented in Fig. 8 (a) and (b), respectively. As shown in Fig. 8 (a), the GFM inverters show similar transients to each other because of the accurate active power sharing among them. When the contingency event is applied, all the GFM inverters increase the active power based on their capabilities and again reach the same frequency. For the reactive power response, as shown in Fig 8 (b), the power sharing is not as accurate, which is as expected because of different voltage drops over the line impedances. In particular, the GFM inverter in CCu7 is negative, which indicates a higher terminal voltage at this inverter, and it needs to absorb reactive power to maintain system voltage stability. Because our focus is to evaluate the stability of the system voltage and frequency, in future research, we will add virtual impedance control to the inverter to achieve more accurate reactive power sharing.

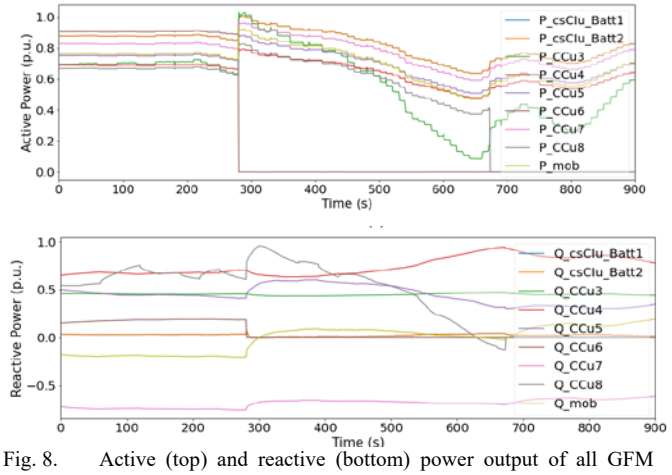

Fig. 8. Active (top) and reactive (bottom) power output of all GFM inverters.

B. Strategy II: Two Battery Inverters in GFM Mode

In this strategy, only two battery inverters (CCu4 and CCu7) are in GFM control, with fixed voltage and frequency references, and the rest of the battery inverters work in droop-based PQ control to inject the desired amount of power. The PQ-controlled battery inverters still use voltage control in the device-level control. To balance power, the battery inverters working in PQ control receive the active power reference equal to 80% of their rated capacity and the reactive power reference equal to 60% of their rated capacity. The integrators in the droop control are enabled to ensure that the DERs closely track their power references.

Fig. 9 (a) and (b) show the frequencies and voltage RMS of each building, respectively. As shown in Fig. 9 (a), the frequencies of all the buildings are maintained near the nominal frequency, 60 Hz. Small jitters are observed in the frequency, which are influenced by the varying load consumption and solar production. The two noticeable drops are caused by the contingency events, with a slightly bigger drop in the second event. This is because only two GFM battery inverters can increase power to compensate for the lost generation, but they do not have enough extra power to do that due to the limited capacity. Fig. 9 (b) shows the voltage RMS of all the buildings. The voltages are maintained near the nominal voltage, 1 p.u. When the contingency events occur, the voltage RMS of each building drops, with the first event causing larger voltage drops due to the loss of a larger generation unit (200 kVA) than the second event (the loss of a generation unit of 50 kVA). Overall, the dynamics of all the voltages in Strategy II are similar to those of Strategy I.

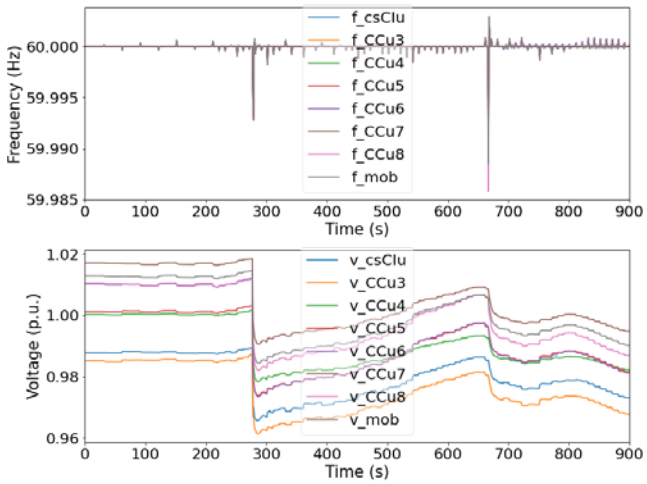

Fig. 9. Frequency (top) and voltage RMS (bottom) of all the buildings.

Next, we explore the active and reactive power output of the two battery GFM inverters, with the rest of the battery inverters operating in PQ control mode. Fig. 10 (a) and (b) show the active and reactive power of the inverters, respectively. As shown in Fig. 10 (a), the two GFM inverters show load-following characteristics, and the rest of the PQ-controlled battery inverters can track the power reference (0.8 p.u.). When the contingency event happens, the two GFM inverters follow the changed net load demand and automatically adjust their output active power. As for the reactive power responses shown in Fig. 10 (b), the two GFM inverters share the power disproportionately with the second GFM inverter, which is absorbing reactive power; the reactive power output of the PQ-controlled battery inverters is maintained near 0.5 p.u., and they cannot accurately track the power reference (0.6 p.u.). When the contingency event happens, the two GFM inverters can follow the changed net load demand and respond accordingly to balance the reactive power demand. Note that the first contingency event causes a significant overshoot in all the inverters.

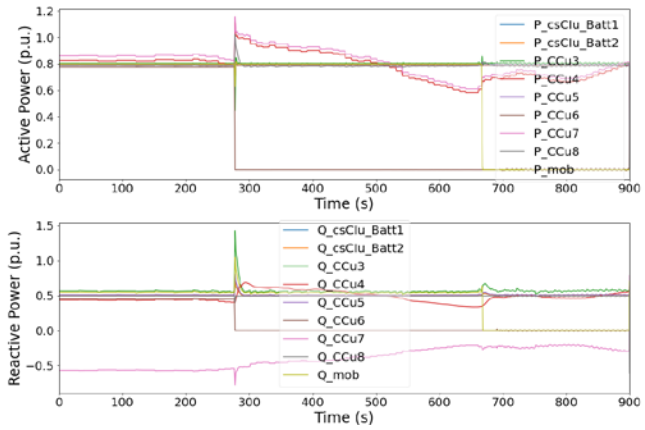

Fig. 10. Active (top) and reactvie (bottom) power output of all the battery inverters.

VI. Conclusions

This paper investigated the stability of a low-inertia microgrid system with many GFM and GFL inverters under two control strategies in which the GFM inverters can choose between GFM and GFL control modes. These two control strategies were evaluated through a real-world campus microgrid system with varying load and solar irradiance profiles. The extensive simulation study shows:

- When changing from at least one GFM inverter in each building to only two GFM inverters in the system, with the rest as GFL inverters (PQ control and current control), the system is unstable. This shows that the GFM inverters maintain better stability than the GFL inverters.
- When the system has only two GFM inverters, any small changes in frequency caused by the power sharing and load following can cause instability. It is not recommended to use only two GFM inverters, with the rest as GFL inverters in PQ and current control; however, the system can be stable if the two GFM inverters use isochronous control to maintain frequency and voltage stability and the GFL inverters use voltage control for PQ control.
- Both strategies can maintain system voltage and frequency stability. Active power sharing is accurate for both strategies, but reactive power sharing is not. In our future work, we will include virtual impedance control to improve the reactive power sharing.
- Strategy I, with more GFM inverters, shows better stability than Strategy II, with fewer GFM inverters, thus demonstrating the benefits of using GFM controls in a microgrid. A microgrid system with a low percentage of GFM inverters can have poor stability but improving the control strategies in the inverters can improve system stability.

This study is applicable for different percentages of GFM inverters. This will be the focus of our future work.

Acknowledgments

The authors thank Soham Chakraborty from the University of Minnesota for providing the network data and model.

References

[1] R. Lasseter, Z. Chen, and D. Pattabiraman, "Grid-Forming Inverters: A Critical Asset for the Power Grid," *IEEE Journal of Emerging and Selected Topics in Power Electronics*, vol. 8, no. 3, June 2020, pp. 925-935.

[2] T. Zhang, "Impacts of Inverter Control Strategies on the Stability of Low-Inertia Power Systems," *IEEE Power and Energy Society General Meeting*, 2020.

[3] J. Wang, "Design Power Control Strategies of Grid-Forming Inverters for Microgrid Application," *IEEE Energy Conversion Congress & Expo (ECCE)*, virtual conference, Oct. 10-14, 2021.

[4] S. Mohiuddin ad J. Qi, "A Unified Droop-Free Distributed Secondary Control for Grid-Following and Grid-Forming Inverters in AC Microgrids," *IEEE Power and Energy Soceity General Meeting*, 2020.

[5] D. Pattabiraman, R. Lassester, and T. Jahns, "Comparison of Grid-Following and Grid-Forming Control for a High Inverter Penetration Power System," *IEEE Power and Energy Society General Meeting*, 2018.

[6] A. Sajadi, R. Kenyon, M. Bossart, and B. Hodge, "Dynamic Interaction of Grid-Forming and Grid-Following Inverters with Synchronous Generators in Hybrid Power Plants," *IEEE Kansas Power and Energy Conference (KPEC)*, 2021.

[7] L. Ding et al., "Region-Based Stability Analysis of Resilient Distribution Systems with Hybrid Grid-Forming and Grid-Following Inverters," *IEEE Energy Conversion Congress & Expo (ECCE)*, virtual conference, Oct. 10-14, 2020.

[8] W. Feng et al., "The Frequency Fluctuation Impact Analysis for Droop-Controlled Grid-Connecting Inverter in Microgrid," *IEEE 8th International Power Electronics and Motion Control Conference (IPEMC -ECCE Asia)*, 2016.

[9] N. Beg, H. Biech, and A. Rosin, "Stability Issues with Inverter Loads and Their Control in Low-Inertia Islanded Microgrids," *IEEE 2nd Global Power, Energy, and Communication Conference*, Oct. 20-23, 2020.

[10] J. Wang, S. Chakraborty, G. Saraswat, and M. Salapaka, "Evaluation of Optimal Net Load Management in Microgrids Using Hardware-in-the-Loop Simulation," *IEEE North American Innovative Smart Grid Technologies*, 2022.

[11] V. Khatana, S. Chakraborty, G. Saraswat, B. Lundstorm, and M. Salapaka, "Evaluation of Horizon of Viability Optimization Engine for Sustained Power to Critical Infrastructure," *2022 IEEE Power and Energy Conference at Illinois (PECI)*, March 2022, pp. 1-8.

[12] J. Wang, N. Chang, X. Feng, and A. Monti, "Design of a Generalized Control Algorithm for Parallel Inverters for Smooth Microgrid Transition Operaiton," *IEEE Tran. Ind. Electron.*, vol. 62, no. 8, Feb. 2015, pp. 4900-4914.

[13] J. Wang, B. Lundstrom, and A. Bernsterin, "Design of a Non-PLL Grid-Forming Inverter for Smooth Microgrid Transition Operation," *IEEE Power and Energy Society General Meeting*, 2020.

[14] J. Wang, Y. Song, and A. Monti, "A Study of Feedforward Control on Stability of Grid-Parallel Inverter with Various Grid Impedance," *IEEE 5th International Symposium on Power Electronics for Distributed Generation Systems (PEDG)*, June 2014.